

LASER-INDUCED GRAPHENE ON PDMS WITH GLYCOL COMPOUNDS AS A POTENTIAL WEARABLE SENSOR

Andela Gavran^{1*}, Marija Pergal¹, Teodora Vićentić¹, Igor A. Pašti^{2,3},
Danica Bajuk-Bogdanović², Marko Spasenović¹

¹ Center for Microelectronic Technologies, Institute of Chemistry, Technology and Metallurgy,
National Institute of the Republic of Serbia, University of Belgrade, Belgrade, Serbia

² University of Belgrade – Faculty of Physical Chemistry, Belgrade, Serbia

³ Serbian Academy of Sciences and Arts, Belgrade, Serbia

* Corresponding author: andjela.gavran@ihmtm.bg.ac.rs

Abstract: Laser-induced graphene (LIG) has been the subject of extensive research over the past decade and has found promising applications in physiological monitoring processes in both sports and medicine. Its excellent characteristics, such as good electrical conductivity, piezoresistivity, flexibility, and low-cost production, make it a suitable material for use in wearable electronics and sensors. Poly(dimethylsiloxane) (PDMS) has attracted attention as a substrate for wearable sensors due to its good biocompatibility, elasticity, and mechanical characteristics. However, since its structure contains no readily carbonizable atoms, PDMS must be modified with glycol additives such as diethylene glycol (PDMS/DEG) and ethylene glycol (PDMS/EG) to enable graphene induction. This paper presents the laser induction of graphene on a PDMS/DEG and PDMS/EG composite, electronic testing, and physicochemical characterization. By optimizing laser parameters, LIG with the lowest electrical resistance was obtained, with PDMS/DEG samples showing superior surface morphology compared to PDMS/EG. Raman spectroscopy revealed the characteristic D, G, and 2D bands typical for graphene. The assignment of bands in infrared spectroscopy (FTIR) and SEM micrographs confirmed the structure of graphene. Characterization revealed that the optimal glycol compound concentration in PDMS is 20 wt.%. In the future, this material has the potential to be used for measuring physiological processes and limb movements.

Keywords: laser-induced graphene, PDMS, sensors, diethylene glycol, ethylene glycol.

1. INTRODUCTION

There is a growing need for wearable devices that are wireless and can measure various physiological parameters, including heart rate, respiration, blood pressure, and limb motion, while reducing their environmental impact [1-4]. In addition, the devices need to be thin, flexible, and highly conductive. Flexible electronic sensors based on laser-induced graphene (LIG) on biocompatible polymers meet all of the above requirements. LIG was first mentioned in 2014 when CO₂ laser irradiation of

polyimide (PI) created a porous graphene structure, which was the focus of numerous research projects over the last decade [5]. LIG exhibited exceptional properties, such as high thermal stability (>900°C), piezoresistance, large surface area (428 m² g⁻¹), and ease of preparation [5-8]. LIG offers a fast and inexpensive method of fabricating flexible portable electronic devices.

Commercially available PI films are the most common precursor for LIG because of their good mechanical stability, high thermal resistance, and

wide availability, but they often require additional surface treatments, such as plasma activation or polymer coatings to improve their biocompatibility in biomedical applications [4,6], and they are also not chemically customizable. Due to the lack of customization options, and poor elasticity of PI, LIG is typically transferred from PI to another substrate or fabricated on a more flexible material. Several studies showed that most carbon-containing materials can be converted into LIG using a CO₂ infrared laser [9,10,11]. Polymers with a chemical structure similar to PI, such as polyetherimide (PEI), poly(ether ether ketone) (PEEK), and polysulfone, were found to be suitable for conversion into LIG [5,12-14]. Poly(dimethylsiloxane) (PDMS) proved to be a favorable substrate for wearable devices due to its good mechanical properties, tunable surface chemistry, low water permeability, excellent thermal stability, low cost, and good biocompatibility [9,15-18]. The main limitation of PDMS lies in its low carbon content, which prevents direct LIG formation. Hence, researchers try to enhance the properties of PDMS by dispersing another polymer or carbon-containing precursor into the PDMS matrix, such as Triton X-100, triethylene glycol (TEG), or poly(ethylene glycol) (PEG) [9,10,19]. Glycol compounds proved to be an excellent carbon source when incorporated into a PDMS matrix, resulting in a high-quality graphene structure [10].

In this study, laser-induced graphene was fabricated on biocompatible, cross-linked PDMS composites incorporating ethylene glycol (EG) and diethylene glycol (DEG). Direct formation of LIG on PDMS/DEG and PDMS/EG substrates was achieved by optimizing laser parameters. The composites were prepared with DEG and EG concentrations ranging from 10 to 40 wt.%. Physicochemical characterization of both composites and the resulting LIG, was carried out using Raman spectroscopy, Fourier-transform infrared (FTIR) spectroscopy, and scanning electron microscopy (SEM) with energy-dispersive X-ray (EDX) analysis. Electrical resistance of LIG-containing samples was also measured. The study identified optimal DEG and EG concentration, as well as laser parameters, for effective graphene induction. The results indicate that these composites represent promising substrates for future wearable sensors intended for monitoring physiological parameters.

2. EXPERIMENTAL SECTION

2.1. Materials

Poly(dimethylsiloxane) (PDMS) prepolymer and curing agent (Sylgard 184, Dow Corning), along with diethylene glycol (DEG) and ethylene glycol (Sigma Aldrich), were used to prepare the PDMS/DEG and PDMS/EG composites.

2.2. Synthesis of PDMS/DEG and PDMS/EG composites

The PDMS prepolymer (α,ω -divinyl poly(dimethylsiloxane), hereafter referred to as PDMS base) was mixed with the curing agent (poly(methyl-hydrogensiloxane), PMHS) in a precise weight ratio of 10:1. Varying amounts of DEG or EG (10, 20, 30, and 40 wt.%) were then added to the mixture, followed by stirring for 15 minutes to ensure homogeneity. The reaction mixture was poured into Petri dishes and degassed in a vacuum-drying chamber for 30 minutes. Materials were cross-linked in an oven at 100 °C for 3 h, followed by an additional vacuum treatment at 50 °C for 5 h to ensure complete cross-linking.

2.3. Laser-induced graphene production and laser parameter optimization strategy

The CO₂ laser used to prepare LIG was a DBK FL-350 with a wavelength of 10.6 μm . The maximum power output of the laser is 60 W, and the resolution was fixed at 1200 DPI. For each DEG and EG concentration (10, 20, 30, 40 wt.%), at least three separate samples were processed, with LIG patterned into square areas (3 mm x 3 mm).

We explored a range of laser power (8.7 - 10.2 W) and scanning speed (35-55 mm s⁻¹), while fixing resolution (1200 DPI). These laser parameters were used to irradiate PDMS composites with 10-40 wt.% DEG and EG concentration. For each set of conditions, we evaluated i) visual appearance (shade of black and continuity of LIG) and ii) electrical resistance (measured at two points across the LIG square with a multimeter).

2.4. LIG characterization

Electrical measurements were conducted using a digital multimeter. The probes were spaced 3 mm apart.

Raman spectra of the materials were recorded using a DXR Raman microscope (Thermo Fisher Scientific, Waltham, MA, USA) with a laser wavelength of $\lambda_l = 532$ nm and a power of 2 mW, focused onto a $2.1 \mu\text{m}$ spot on the surface. Three measurements at different positions on each sample were performed (10 exposures, 10 seconds each per position). The crystallite size along the a-axis (L_a) was calculated using the Tuinstra and Koenig equation as follows [20,21]:

$$L_a = (2.4 \cdot 10^{-10}) \cdot \lambda_l^4 \cdot \left(\frac{I_D}{I_G}\right)^{-1} \quad (1)$$

In equation (1), the ratio I_D/I_G represents the ratio between the intensity of the D band and the G band.

SEM combined with EDX (Phenom, Thermo Fisher Scientific, Waltham, MA, USA) was employed to analyze material morphology and chemical composition. Sample preparation was not required for SEM and EDX analysis.

FTIR spectra of PDMS/DEG, PDMS/EG, and powdered LIG, obtained by scraping from composites, were recorded in transmission mode on KBr substrates using an FTIR spectrophotometer (Thermo Fisher Scientific, Waltham, MA, USA). All spectra were collected in the range from 4000 to 400 cm^{-1} , with a resolution of 4 cm^{-1} and 32 scans for each sample.

3. RESULTS AND DISCUSSION

3.1. Polymer synthesis

Eight cross-linked PDMS composites containing different amounts of EG and DEG (10–40 wt.%) were synthesized by hydrosilylation. Cross-linking occurs between the vinyl groups of the PDMS base and the Si–H groups of the curing agent. The scheme of polymer synthesis and LIG formation is depicted in Figure 1.

3.2. Electrical characterization of LIG on PDMS/EG and PDMS/DEG

The PDMS/EG and PDMS/DEG composites were irradiated with a CO_2 laser, where visual appearance and electrical resistance were the main factors for choosing the optimal samples for characterization. Electrical resistance measurements for LIG on PDMS/DEG showed that the lowest resistance of $\sim 14 \text{ k}\Omega$ was measured on a LIG made with 9 W of laser power, 45 mm s^{-1} of laser speed, and a 1200 DPI resolution. For the LIG on PDMS/EG, electrical resistance measurements showed that the lowest resistance of $\sim 30 \text{ k}\Omega$ was measured for LIG made with 8.7 W of laser power, 55 mm s^{-1} of laser speed, and a 1200 DPI resolution. These values indicate moderate electrical conductivity, typical of LIG structures produced directly on polymeric substrates [9,10].

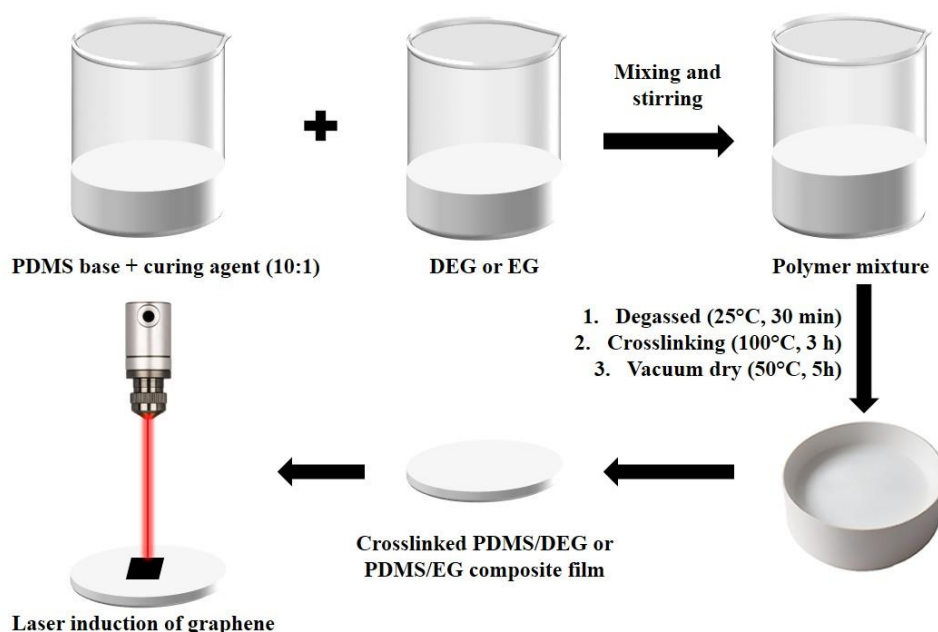


Figure 1. The scheme of polymer synthesis and LIG fabrication.

3.3. Raman spectroscopy

Figure 2 depicts the most representative Raman spectra of LIG on PDMS substrate with 10-40 wt.% DEG concentration. The ratio of the intensity of the D to the G peaks and 2D to the G peaks, full width at half maximum (FWHM), and crystallite size (L_a) as a function of DEG concentration were analyzed (Figure 2a, 2b, 2c, and 2d, respectively). All spectra are taken from LIG produced with 9 W of laser power, a resolution of 1200 DPI, and a scanning speed of 45 mm s⁻¹. Raman spectra of LIG on PDMS/DEG composites show three prominent peaks char-

acteristic of graphene: the D band (~1346 cm⁻¹) related to defects in sp² carbon domains, the G band (~1581 cm⁻¹) assigned to the E_{2g} vibration of sp²-hybridized carbon atoms, and a 2D band at ~2700 cm⁻¹ that originates from the second-order mode of the D peak [5]. Although Raman spectra of LIG on PDMS with 10 wt.% and 20 wt.% DEG concentration shows intense D and 2D peaks, in the spectra of other samples, the bands are not obvious.

Spectral deconvolution was performed to obtain I_D/I_G , I_{2D}/I_G (using the surface below peaks), and FWHM, and we calculated L_a using the Tuinstra and Koenig equation. Results are presented in Table 1.

Table 1. Intensity ratio of D and G, and 2D and G band for LIG on PDMS/DEG made with a 9 W of laser power and a scanning speed of 45 mm s⁻¹.

Materials	I_D/I_G	I_{2D}/I_G	FWHM (cm ⁻¹)		L_a (nm)
			D	G	
LIG/PDMS/10%DEG	0.50	1.30	42.4	35.8	38.1
LIG/PDMS/20%DEG	0.46	1.36	42.5	34.6	42.1
LIG/PDMS/30%DEG	1.99	0.23	108.9	64.3	9.6
LIG/PDMS/40%DEG	1.24	0.09	84.8	78.2	15.4

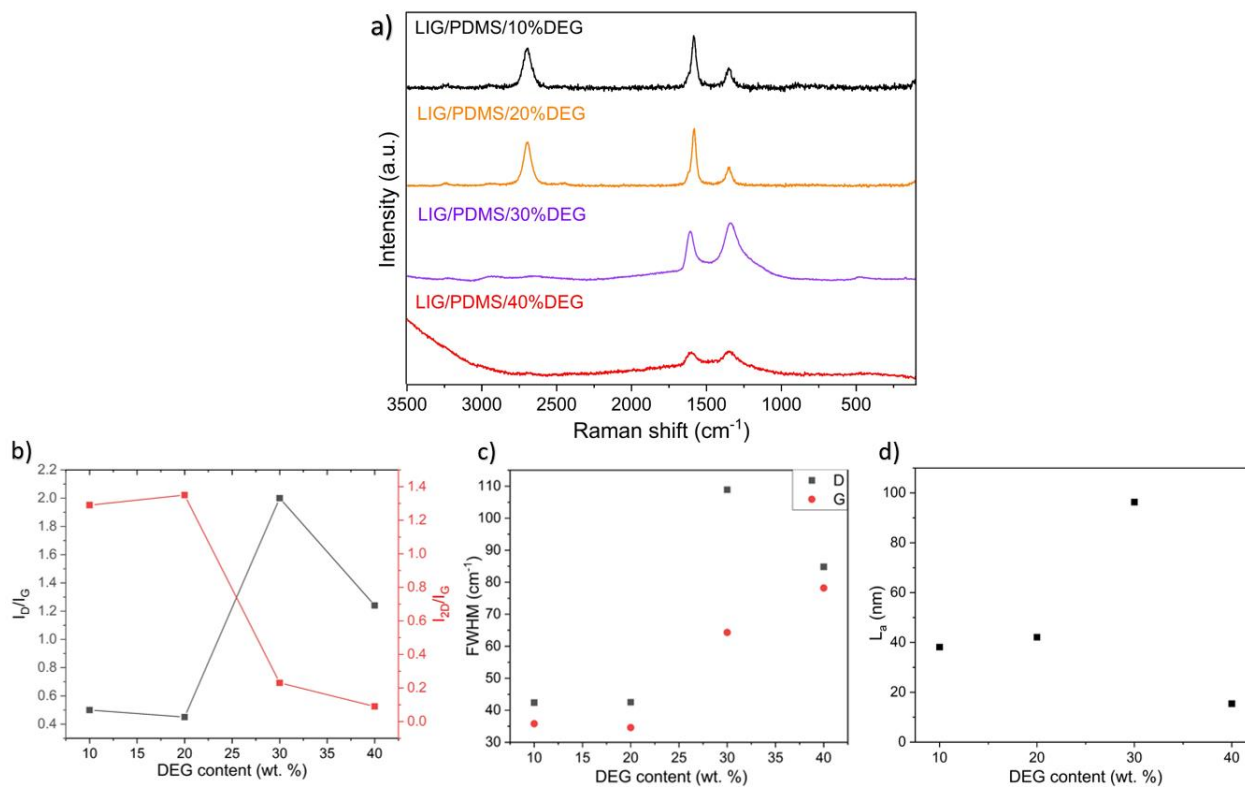


Figure 2. a) Raman spectra of representative samples of LIG on PDMS with various DEG concentration; b) I_D/I_G and I_{2D}/I_G as a function of DEG concentration; c) FWHM as a function of DEG concentration; d) L_a as a function of DEG concentration.

The ratio of the intensity of the D to the G peaks for LIG on PDMS/10%DEG and PDMS/20%DEG is smaller than 1, suggesting the lowest concentration of defects [22]. I_{2D}/I_G ratio was around 1, which is common for bilayer graphene [23]. FWHM as a measure of structural disorder shows that low FWHM values for the D and G peaks at DEG concentration of 10 wt.% and 20 wt.% suggest low-disordered material [24]. In contrast, samples containing 30 wt.% and 40 wt.% DEG exhibited higher I_D/I_G and broader peaks, consistent with amorphous or highly disordered carbon structures. The values used were the best from three positions on each sample where Raman spectra were recorded.

Figure 3 depicts the most representative Raman spectra of LIG on PDMS with 10-40 wt.% EG concentration, including the ratio of the intensity of the D to the G peaks, the 2D to the G peaks, the full width at half maximum (FWHM), and crystallite size (L_a) as a function of EG content (Figure 3a, 3b, 3c, and 3d, respectively). All spectra are taken from LIG produced with 8.7 W of laser power, a resolution of 1200 DPI, and a scanning speed of 55 mm s⁻¹. Similar to the Raman spectra of LIG/PDMS/DEG,

spectra of LIG on PDMS/EG composites show the same three peaks characteristic of graphene. Raman spectra of LIG on PDMS with 10 wt.% and 20 wt.% EG concentration similar to Raman spectra of LIG on PDMS with 10 wt.% and 20 wt.% DEG concentration shows intense D and 2D peaks. In contrast to that, Raman spectra of LIG on PDMS with 30 wt.% and 40 wt.% EG concentration show D and G peaks of similar intensity and a small 2D peak, suggesting that more oxidized or disordered graphene formed on those samples.

Spectral deconvolution was performed to obtain I_D/I_G , I_{2D}/I_G , and FWHM, and we calculated L_a with the Tuinstra and Koenig equation. The results are presented in Table 2. The ratio I_D/I_G for LIG on PDMS/10%EG and PDMS/20%EG is smaller than 1, and the I_{2D}/I_G is around 1, like in the case of LIG/PDMS/DEG, suggesting again the lowest concentration of defects and formation of bilayer graphene [22,23]. Quantitative analysis (Table 2) revealed that I_D/I_G ratios for LIG on PDMS/EG (average ~1.31) were lower than those on PDMS/DEG (average ~1.8), indicating fewer structural defects in EG-based composites. Moreover, the largest

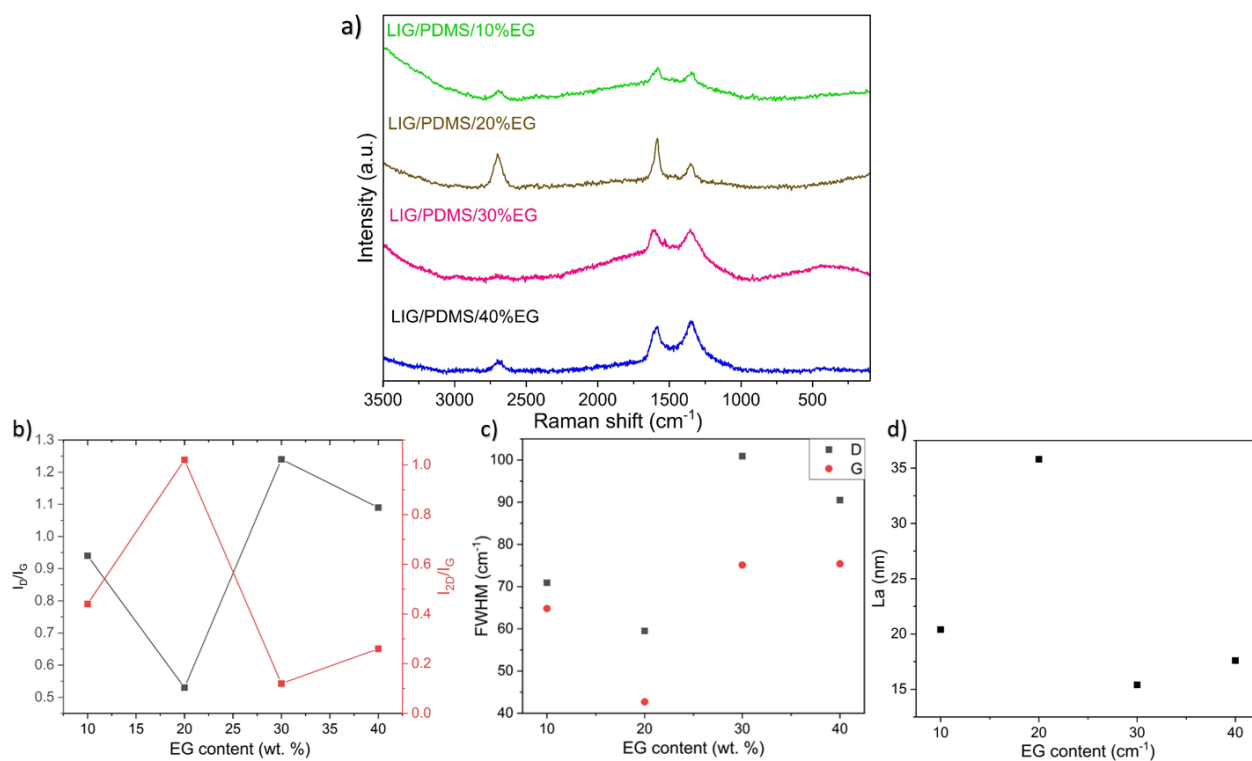


Figure 3. a) Raman spectra of representative samples of LIG on PDMS with various EG concentration; b) I_D/I_G and I_{2D}/I_G as a function of EG concentration; c) FWHM as a function of EG concentration; d) L_a as a function of EG concentration.

crystallite size ($L_a = 35.8$ nm) was observed for LIG on PDMS/20%EG, consistent with the formation of well-defined graphene domains [19]. At higher EG concentration (30–40 wt.%), increased I_D/I_G and broadened FWHM values pointed to a higher degree of disorder, corroborating the visual and electrical results. At 30–40 wt.% EG, the material became significantly more defective: I_D/I_G rose to 1.1–1.25, I_{2D}/I_G dropped to 0.12–0.27, and FWHM of G broadened to 75 cm^{-1} , indicating oxidation and amorphization of the carbon framework. The values used were the best of the three positions where Raman spectra were recorded.

Table 2. Intensity ratio of D and G, and 2D and G band for LIG on PDMS/EG made with an 8.7 W of laser power and a scanning speed of 55 mm s^{-1} .

Materials	I_D/I_G	I_{2D}/I_G	FWHM (cm^{-1})		L_a (nm)
			D	G	
LIG/PDMS/10%EG	0.94	0.45	70.9	64.8	20.4
LIG/PDMS/20%EG	0.54	1.03	59.5	42.7	35.8
LIG/PDMS/30%EG	1.25	0.12	100.9	75.1	15.4
LIG/PDMS/40%EG	1.10	0.27	90.3	75.4	17.6

3.4. FTIR spectroscopy

FTIR spectra of PDMS/DEG and PDMS/EG composites (10 and 40 wt.%) and their corresponding LIG samples are presented in Figure 4. A broad band at $\sim 3400\text{ cm}^{-1}$, attributed to O–H stretching vibrations, was pronounced in DEG-rich composites but much weaker in EG-based ones compared to the remaining spectral features.

Strong absorptions near 2900 and 2960 cm^{-1} (ν_{as} and ν_{s} CH₂) were evident in the pristine composites but strongly reduced after laser irradiation, reflecting the removal of aliphatic groups during carbonization. A weak band near 1600 cm^{-1} , absent in pristine PDMS, may arise from secondary reactions of EG/DEG with PDMS or partially oxidized carbon domains [10].

The expected graphenic C=C stretching near 1630 cm^{-1} was not clearly detected in LIG spectra. This absence is explained by the dominance of a broad, intense band centered near 1100 cm^{-1} , attributed to Si–O–Si and SiO₂ nanoparticles formed by

PDMS decomposition under high-temperature CO₂ laser irradiation [7,10]. This overlap masks weaker C=C contributions. A low-intensity peak near 1400 cm^{-1} (C–H deformation) was observed only in LIG/PDMS/DEG. Bands below 1200 cm^{-1} , especially at $840\text{--}860\text{ cm}^{-1}$ (–CH₃ rocking in Si–CH₃), remained prominent in composites and can indicate that Si–C is formed due to the thermal degradation of the PDMS matrix [10].

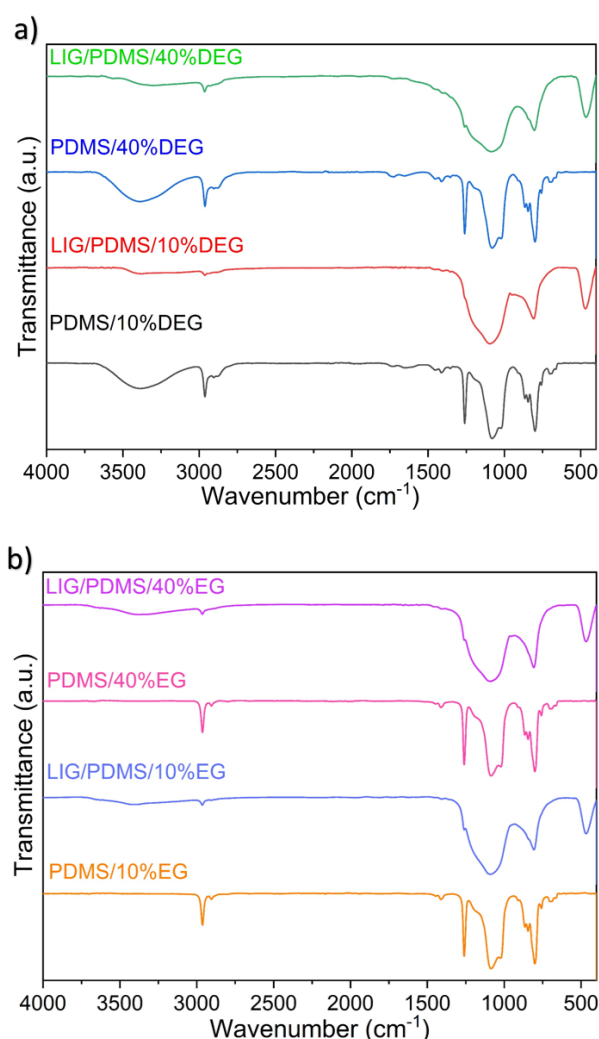


Figure 4. a) FTIR spectra of PDMS with 10 and 40 wt.% DEG, and LIG on PDMS with 10 and 40 wt.% DEG; b) FTIR spectra of PDMS with 10 and 40 wt.% EG, and LIG on PDMS with 10 and 40 wt.% EG concentrations.

3.5. SEM-EDX

Figure 5 depicts SEM micrographs of the cross-section of LIG on PDMS/DEG (Figure 5a) and PDMS/EG (Figure 5b) composites with 20

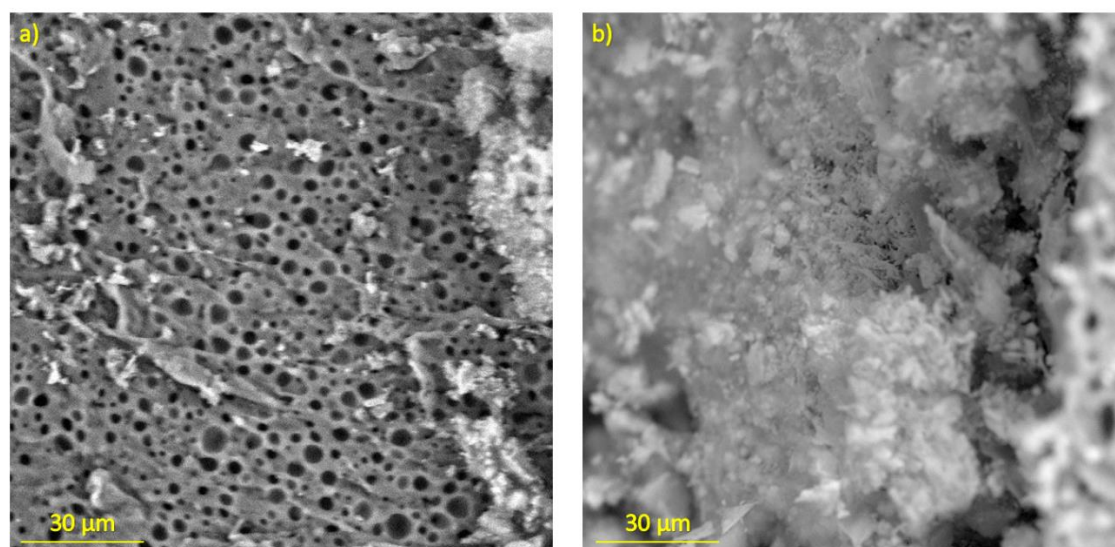


Figure 5. SEM micrographs of a) LIG/PDMS/20%DEG and b) LIG/PDMS/20%EG with 2000x magnification.

wt.% glycol concentration, chosen for their optimal quality as judged from Raman spectra. For the LIG/PDMS/20%DEG, laser parameters were 9 W of laser power, scanning laser speed 45 mms^{-1} and resolution of 1200 DPI, and for the LIG/PDMS/20%EG, laser parameters were 8.7 W, 55 mm s^{-1} laser speed, and 1200 DPI resolution. Porous, foam-like morphology was more pronounced in DEG-based samples.

EDX analysis showed the elemental composition of LIG in both samples. Both samples show high concentrations of carbon, which suggests the formation of LIG [3,19,20]. For LIG on PDMS/DEG, the atomic concentrations of C, Si, and O are 37.8%, 23.7%, and 38.4%, respectively. For LIG on PDMS/EG, the atomic concentrations of C, Si, and O are 45.4%, 21.8%, and 32.7%, respectively. The higher carbon fraction and reduced oxygen content in EG-based samples support more efficient carbonization, in agreement with Raman results showing low I_D/I_G values at 20 wt.% EG.

4. CONCLUSION

In this work, we demonstrated the successful laser induction of graphene on novel biocompatible PDMS/DEG and PDMS/EG composites. Systematic physicochemical characterization by Raman, FTIR, and SEM-EDX confirmed the formation of laser-induced graphene and provided insight into the role of glycol additives modifiers in tailoring their properties. The lowest electrical resistance ($\sim 14 \text{ k}\Omega$) was

obtained for LIG on PDMS/DEG fabricated at 9 W laser power, 45 mm s^{-1} scanning speed, and 1200 DPI resolution, while LIG on PDMS/EG exhibited the lowest resistance ($\sim 30 \text{ k}\Omega$) at 8.7 W, 55 mm s^{-1} , and 1200 DPI. These values reflect moderate conductivity, typical for LIG produced on polymeric matrices [9,10].

Raman spectroscopy revealed the characteristic D, G, and 2D bands of graphene. Low I_D/I_G ratios and narrow FWHM values at 10–20 wt.% ethylene glycol compound content indicated reduced defect density and improved graphene ordering. Comparative analysis showed that LIG on PDMS/EG exhibited fewer defects and larger crystallite sizes than LIG on PDMS/DEG, suggesting that EG is a more effective modifier for promoting graphene formation. Excessive loading of DEG and EG (30–40 wt.%) in PDMS led to structural degradation and poor-quality LIG. FTIR spectra provided additional supporting evidence of LIG formation, although certain characteristic peaks overlapped with those originating from SiO_2 nanoparticles formed during thermal decomposition of PDMS. SEM revealed the porous morphology typical of LIG, while EDX confirmed increased carbon content, with $\sim 45\%$ for EG-based composite and $\sim 38\%$ for DEG-based composite.

Overall, the results demonstrate that PDMS/DEG and PDMS/EG composites are promising candidates for flexible substrates in wearable electronics. Future work will focus on more comprehensive physicochemical characterization, optimization of

electrical and mechanical properties, and the integration of these composites into wearable sensors for biomedical and sports applications.

5. ACKNOWLEDGMENT

This research was supported by the Science Fund of the Republic of Serbia, #4950, Polymer/graphene heterostructures for physiological sensors—Polygraph. The authors also would like to thank the Ministry of Science, Technological Development, and Innovation of the Republic of Serbia (Contract No: 451-03-136/2025-03/200026 and 451-03-65/2024-03/200146).

6. REFERENCES

- [1] Huang L. et al., *Flexible capacitive pressure sensor based on laser-induced graphene and polydimethylsiloxane foam*, IEEE Sens., J., 21, (2021) 12048–12056.
- [2] Ma Z., Khoo B. L., Recent advances in laser-induced-graphene-based soft skin electronics for intelligent healthcare. *Soft Sci.*, 4, (2024) 26.
- [3] Vićentić T. et al., *Laser-Induced Graphene for Heartbeat Monitoring with HeartPy Analysis*. Sensors, 22, 17, (2022) 6326.
- [4] Mamleyev E.R. et al., *Laser-induced hierarchical carbon patterns on polyimide substrates for flexible urea sensors*. npj Flex. Electron., 3, 2, (2019) 1-11.
- [5] Lin J. et al., *Laser-induced porous graphene films from commercial polymers*. Nat. Commun., 5, (2014) 5714.
- [6] Carvalho A.F. et al., *Laser-induced graphene piezoresistive sensors synthesized directly on cork insoles for gait analysis*. Adv. Mater. Technol., 5, (2020) 2000630.
- [7] Zhang C., Ping J., Ying Y., *Evaluation of trans-resveratrol level in grape wine using laser-induced porous graphene-based electrochemical sensor*. Sci. Total Environ., 714, (2020) 136687.
- [8] Hong S. et al., *Surface morphological growth characteristics of laser-induced graphene with UV pulsed laser and sensor applications*. ACS Matter. Lett., 5, 4, (2023) 1261-1270.
- [9] Pergal M. V. et al. *Laser-Induced Graphene on Novel Crosslinked Poly(dimethylsiloxane)/Triton X-100 Composites for Improving Mechanical, Electrical and Hydrophobic Properties*. Polymers, 16, (2024) 3157.
- [10] Gavran A. et al., *Laser-induced graphene on novel biocompatible PDMS/PEG substrate for limb motion sensors*, Sensors, 25, 17, (2025) 5238.
- [11] Vojnović V. et al., *Pulse Sensors Based on Laser-Induced Graphene Transferred to Biocompatible Polyurethane Networks: Fabrication, Transfer Methods, Characterization, and Application*. Chemosensors, 13, (2025) 122.
- [12] Tang, L. et al., *Laser-Induced Graphene Electrodes on Poly(ether-ether-ketone)/PDMS Composite Films for Flexible Strain and Humidity Sensors*. ACS Appl. Nano. Mater., 6, 19, (2023) 17802-17813.
- [13] Singh S. P. et al., *Sulfur-doped laser-induced porous graphene derived from polysulfone-class polymers and membranes*. ACS Appl. Nano Mater., 12, 1, (2018) 289-297.
- [14] Yazdi, A.Z. et al., *Direct Creation of Highly Conductive Laser-Induced Graphene Nanocomposites from Polymer Blends*. Macromol. Rapid Commun., 38, (2017) 1700176.
- [15] Kim T. K., Kim J. K., Jeong, O. C., *Measurement of nonlinear mechanical properties of PDMS elastomer*. Microelectron. Eng., 88, 8, (2011) 1982-1985.
- [16] Pinho D. et al., *Flexible PDMS microparticles to mimic RBCs in blood particulate analogue fluids*. Mech. Res. Commun., 100, (2019) 103399.
- [17] Lötters, J. C. et al., *The mechanical properties of the rubber elastic polymer polydimethylsiloxane for sensor applications*. J. Micromech. Microeng., 7, 3, (1997) 145.
- [18] Heo B. et al., *A low-cost, composite collagen-PDMS material for extended fluid retention in the skin-interfaced microfluidic devices*. Colloids Interface Sci. Commun., 38, (2020) 100301.
- [19] Zaccagnini, P. et al., *Laser-induced graphenization of PDMS as flexible electrode for micro-supercapacitors*. Adv. Mater. Interfaces, 8, 23, (2021) 2101046.
- [20] Ferrari A. C., Robertson J., *Interpretation of Raman Spectra of Disordered and Amorphous Carbon*. Phys. Rev B., 61, (2000) 14095.
- [21] Parmeggiani M. et al., *PDMS/Polyimide Composite as an Elastomeric Substrate for Multifunctional Laser-Induced Graphene Electrodes*.

- ACS Appl. Mater. Interfaces, 11, 36, (2019) 33221–33230.
- [22] Yan Z. et al., *Growth of Bilayer Graphene on Insulating Substrates*, ACS Nano, 5, 10, (2011) 8187–8192.
- [23] Scardaci V.; Compagnini G., *Raman spectroscopy data related to the laser induced reduction of graphene oxide*. Data Brief, 38, (2021) 107306.
- [24] Ayman Y. et al., *FT-IR Spectroscopy for the Detection of Diethylene Glycol (DEG) Contaminant in Glycerin-Based Pharmaceutical Products and Food Supplements*, Acta Chim. Slov., 67, 2, (2020) 530.

ЛАСЕРСКИ ИНДУКОВАН ГРАФЕН НА ПДМС-У СА ГЛИКОЛНИМ ЈЕДИЊЕЊИМА КАО ПОТЕНЦИЈАЛНИ НОСИВИ СЕНЗОР

Сажетак: Ласерски-индукован графен (LIG) је постао тема бројних истраживања у последњих десет година, са значајном применом у праћењу физиолошких процеса области спорта и медицине. Његова својства као што су добра електрична проводљивост, пиезорезистивност, флексибилност и ниски трошкови производње га чине погодним материјалом за примену у носивој електроници и сензорима. Поли(диметилсилоксан) (PDMS) је привукао пажњу као супстрат за носиве сензоре због своје добре биокompatбилности, еластичности и механичких својстава. Међутим, због малог удела угљеникових атома у њему, потребно је модификовати га са гликолним једињењима богатим угљеником као што су ди(етилен гликол) (PDMS/DEG) и етилен гликол (PDMS/EG). У овом раду је представљена ласерска индукција графена на полимерним композитима PDMS/DEG и PDMS/EG-а, електронска испитивања и физичко-хемијска карактеризација. Оптимизацијом ласерских параметара је постигнут LIG са најнижом електричном отпорношћу, где узорци LIG-а на PDMS/DEG-у имају бољу површинску морфологију од узорака на PDMS/EG. У раманским спектрима уочавају се траке Д, Г и 2Д, карактеристичне за графен. Анализа ИЦ спектра, као и асигнација трака у инфрацрвеној спектроскопији и скенирајућа електронска микроскопија су потврдили структуру графена. На основу свих резултата испитивања новог материјала показано је да је оптимална концентрација гликолних једињења у PDMS-у 20 мас.%. У будућности, овај материјал има потенцијал да буде коришћен у сврхе мерења физиолошких процеса и покрета удова.

Кључне речи: ласерски-индукован графен, поли(диметилсилоксан), диетилен гликол, етилен гликол.

Paper received: 1 September 2025

Paper accepted: 30 March 2026



This work is licensed under a Creative Commons Attribution-NonCommercial 4.0 International License